Detector Assessment for 1D Single-Shot Spontaneous Raman Scattering for Temperature and Multi-Species Measurements in Flames

H. Ajrouche, A. Lo, P. Vervisch, A. Cessou

Detector Assessment for 1D Single-Shot Spontaneous Raman Scattering for Temperature and Multi-Species Measurements in Flames

H. Ajrouche [1], A. Lo[1], P. Vervisch[1], A. Cessou[1,*]
1: CORIA-UMR6614, Normandie Université, CNRS, INSA et Université de Rouen, France
* Correspondent author: Armelle.cessou@coria.fr

Keywords: Spontaneous Raman Scattering, Temperature, species number density, Combustion

ABSTRACT

The critical aspect of 1D single-shot Spontaneous Raman Scattering (SRS) experiments in flames is the requirement of high efficiency of the detection system associated with a fast temporal gating. Single-shot SRS measurements in flames are performed either with ICCD or with back-illuminated CCDs associated with a fast shutter. Two types of back-illuminated CDD detectors are used: a back-illuminated CCD (BI-CCD) and electron multiplying CCD (BI-EMCCD). The purpose of the present paper is to compare the three detectors: the ICCD with its intensifier gating and the back-illuminated CCDs with a Pockels cell shutter developed in a previous work (Ajrouche et al, 2015). The accuracy and uncertainty of 1D single-shot SRS measurements of temperature and density are quantified in near-adiabatic CH4/air flames. This is performed for N_2 number density (high signal levels), and CO number density (low signal levels) corresponding to signal close to the detectability limit. The temperature is determined by modeling the vibration-rotation spectra of N_2 offering advantage of not requiring reference temperature and the modeled spectra are used as smoothed spectra to determine the instantaneous number densities. On one hand, the BI-CCD with the Pockels cell shutter is the most efficient detection systems in extreme low light situations for single-shot temperature measurements, and on the other hand the BI-EMCCD is the most powerful tool for best detectability of low density species.

1. Introduction

Validation of theoretical and numerical combustion models has motivated the development of Spontaneous Raman Scattering (SRS) as a multispecies diagnostic (Barlow 2007, Gabet et al. 2010). Due to its low efficiency, turbulent flame investigation by SRS is most of the times limited to 1D measurements even if few works of imaging are proposed (Kelman and Masri 1997), and it requires on one hand high laser energies, greater than 1J/pulse (Meier and Keck 2002), associated with long pulse duration to avoid optical breakdown (Cleon et al. 2007), and on the other hand very sensitive detectors. Moreover, the weak SRS is usually embedded in the flame emission, thus an efficient detection system is required, not only with high efficiency (high sensitivity, low noise,

high dynamic range) but also with a fast temporal gating. Thus the critical aspect of 1D single-shot Spontaneous Raman Scattering (SRS) experiments in flames is the requirement of high efficiency of the detection system associated with a fast temporal gating.

In the present work, the potential applicability and the limitation of three detector types are analyzed for instantaneous 1D Raman measurements of temperature and species concentrations in flames: back-illuminated CCD (BI-CCD), electron multiplying CCD (BI-EMCCD) and intensified CCD (ICCD). Single-shot SRS measurements in flames are usually performed either with BI-CCD (Fernandez et al. 2006) associated with a home-made shutters (Kojima and Nguyen 2008, Miles 2000) or with ICCD cameras (Geyer et al. 2005). The advantage of each solution is the high sensitivity for BICDD and fast gating for ICCD. Their main drawback is the requirement of developing a shutter for BI-CCD and the high shot-noise for ICCD. Back-illuminated cameras require a fast shutter, due to their full-frame architecture. Without fast shutters, the pixels may be exposed during the readout time, causing smearing, especially when the camera is placed in front of a luminous medium like flames. The electron multiplying CCD camera (EMCCD), which have extremely high quantum efficiency (QE) when back-illuminated (BI-EMCCD), offers the ability to eliminate the readout noise detection limit (Gregor and Dreizler 2009) but keeps the need for a fast shutter. We have previously proposed a new fast shutter for 1D single-shot measurements of temperature and concentration of major species by SRS (Ajrouche et al. 2015), where the ability of a Pockels cell shutter (PCS) to enhance the signal-to-noise ratio (SNR) has been demonstrated. This fast shutter is used to assess the ability to measure single-shot scalar values accurately in flames by comparing the BI-CCD, BI-EMCCD and ICCD detection systems. The assessment of the detectors is performed by comparing measurements performed in near-adiabatic CH4/air flames. First, the SNR of these detectors is compared. Second, the accuracy and uncertainty of temperature measurements by SRS, with a procedure presented in previous work (Lo et al. 2012), are analyzed for each detector used and compared to adiabatic 1D freely propagating laminar flames modeling. Third, 1D single-shot density measurements of the 3 detectors are compared for N_2 number density quantified when crossing the flame front and for density corresponding to signals close to the detectability limit by probing CO in a near-stoichiometric rich premixed flame.

2. Experimental setup

Fig. 1 shows the layout of the SRS set-up. The laser source consists in a Nd:YAG laser (Agilite Continuum) operating at 10 Hz providing about 1.2 J with top-hat pulse with a long pulse duration adjustable from 200 ns till 1 μs. A long pulse duration provides a large energy deposit suitable for single-shot SRS (Meier and Keck 2002), with good spatial resolution and without optical

breakdown due to instantaneous and local irradiance is smaller than threshold value of 34 GW/cm² (Cleon, Stepowski and Cessou 2007). The pulse duration used in this study is 310 ns. The laser beam is focused using a convergent lens with a 1 m focal-length providing a probe volume of 170 µm- thick (1/e²). The SRS light is collected at right angle to the laser beam with a large solid angle (f/2) using two telescopes composed of achromatic lenses. The scattered light at the laser wavelength is rejected by a notch filter (HNPF-18702, Kaiser Optical System, OD=6, FWHM 20 nm, transmission efficiency in passbands >80%) placed in the second collimated part of the optical collection system. Then, a periscope is used to rotate the image of the laser beam parallel to the entrance slit of the spectrograph.

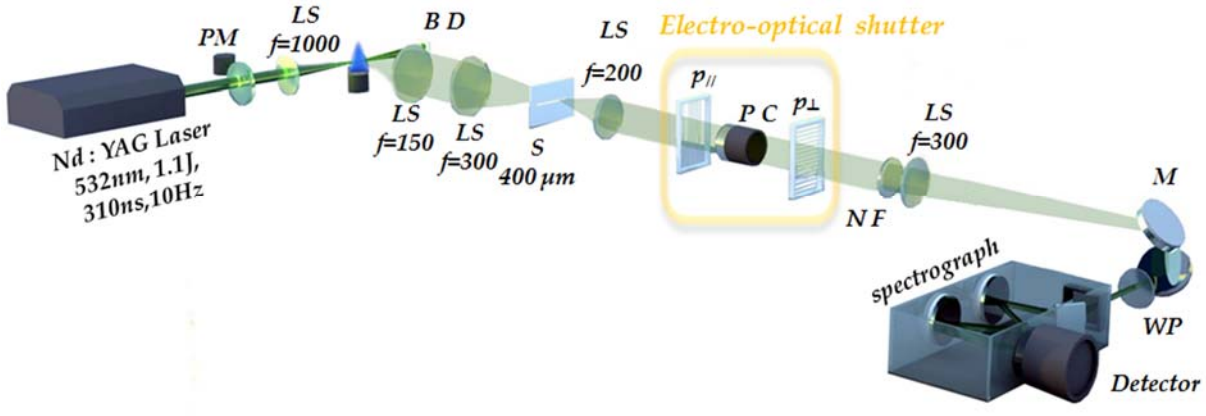

Fig. 1 Overview of the experimental set-up: S, slit; LS, Lens (AR coated @400-700nm) PC, Pockels Cell; P, Polarizer; BD, beam dump; PM, Power meter; NF, Notch filter (532 nm, FWHM 20 nm); WP, half-wave plate

In this study, three types of camera are compared with different quantum efficiency (QE) and noise factor (NF), which originates from the amplification process, defined as the ratio of the output noise of the amplifier to the product of the multiplication gain by the input noise. An ideal amplifier has therefore a noise factor of 1. The consequence of the stochastic nature of the gain in both BI-EMCCDs and ICCDs is a fundamental parameter affecting the SNR.

The ICCD detector used is a 16 bit CCD camera equipped with a GenIII intensifier (PI-MAX UNIGEN, Princeton Instruments, 512 x 512pixels, pixel size 23µm, readout rate of 1 MHz). The maximal QE provided by this device is 38% between 400 and 700 nm. The image intensifier was operated in gated mode with a gate width of 500 ns, suitable to suppress non-laser-induced emissions, such as flame luminosity.

The back-illuminated CCD camera is a full-frame CCD (Pixis 400B, Princeton Instruments, 1340x400 pixels, pixel size 20 µm, NF=1). This camera offers approximately 94 % of QE with 16-bits of dynamic range and readout noise (<13e-). Different analog-to-digital converters (ADC) are

available as 1-2 MHz or 100 KHz. Because the readout noise of CCD arrays increases with the readout rate, the 100 KHz ADC is chosen to enhance the SNR.

The last camera is a back-illuminated electron-multiplying CCD camera (BI-EMCCD) (ProEM, Princeton Instruments, 1600x200pixels, pixel size 16 μm, 94% of QE). The selected EM gain setting was approximately (x200) and was sufficient to make the readout noise negligible. The readout rate used in this study is 1MHz. A fast electro-optical shutter is used for SRS measurements in flame with the two non-intensified detectors (BI-CCD or BI-EMCCD). The PCS consists of a large aperture Pockels cell (LAP-50, KD*P, 50 mm aperture, Quantum Technology) between 2 crossed polarizers (19WG-50, Quantum Technology). The two crossed wire-grid polarizers have high transmission (85% of the polarized incident light for each polarizer) leading to PCS transmission of about 72% of the Raman signal (Ajrouche, Lo, Vervisch and Cessou 2015). With the PCS switched on, the flame emission is integrated on a small time interval (500 ns), and its contribution on the spectra becomes negligible. After the PCS, an achromatic half-wave plate (AHWP10M-600, THORLABS) is placed in front of the spectrograph and oriented in order to obtain the best efficiency of the spectrograph.

3. Results and discussion

Single-shot SRS temperature and multispecies measurements from BI-CCD, BI-EMCCD and ICCD are compared by measurements in a premixed laminar flame, stabilized downstream a Bunsen burner fed with a methane-air mixture with equivalence ratios of Φ=1 and 1.4. The measurements are performed at two locations (Figure 2): in burnt gas downstream the flame tip (GB) and along a profile from fresh gas to burnt gas crossing the flame front (GF). GB is located in a region of homogeneous temperature and composition, close to equilibrium conditions. Measurements in GF offer measurements in various conditions: fresh mixture near the centerline, homogeneous burnt gas at the periphery, and sharp temperature and composition gradient for the intermediate radii, when crossing the preheat and reaction zone. Since the laser beam does not cross the flame front perpendicularly, the experimental profiles are corrected from the angle effect assuming that the tangential temperature gradients are negligible at the height probed, far from the flame tip and burner lip. The measurements are compared to modeling calculation of 1D freely propagating laminar flame by the COSILAB (COSILAB 2007) software, using the GRI-Mech 3.0 chemical mechanism. In first approximation the stretch effect on the temperature and species profiles are neglected. This assumption will be discussed afterwards. In the following, the COSILAB modeling will be considered to provide the reference data (temperature and major species) of the flame.

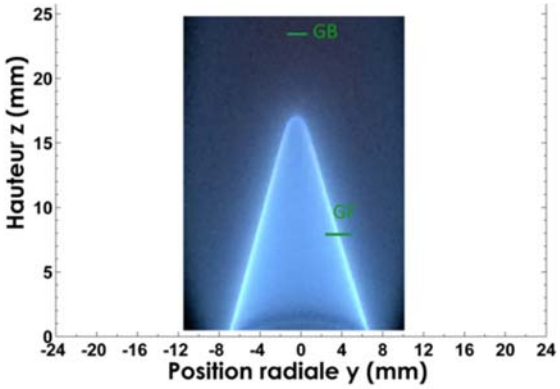

Fig. 2 photo of the CH4-air flame and locations of the SRS measurements (GB) and (GF)

Most of the measurements are performed at Φ=1, for which the adiabatic temperature determined by modeling is 2136 K. The Φ=1.4 flame is used to assess the cameras for measuring low level of concentrations, especially in probing CO which is a species difficult to probe by SRS in flame (Barlow et al, 2009). The experimental spectra are fitted by theoretical spectra by the procedure described by Lo et al (Lo, Cléon, Vervisch and Cessou 2012). From this procedure instantaneous temperature can be measured (Ajrouche, Lo, Vervisch and Cessou 2014). Figure 3 shows the temperature measurements across the flame front obtained from the average spectra collected by the three detectors. Despite the difference of the apparatus functions illustrating by the N_2 SRS peak (Fig.3, right), the temperature profiles illustrate how the procedure developed provides accurate and reproducible temperature measurements.

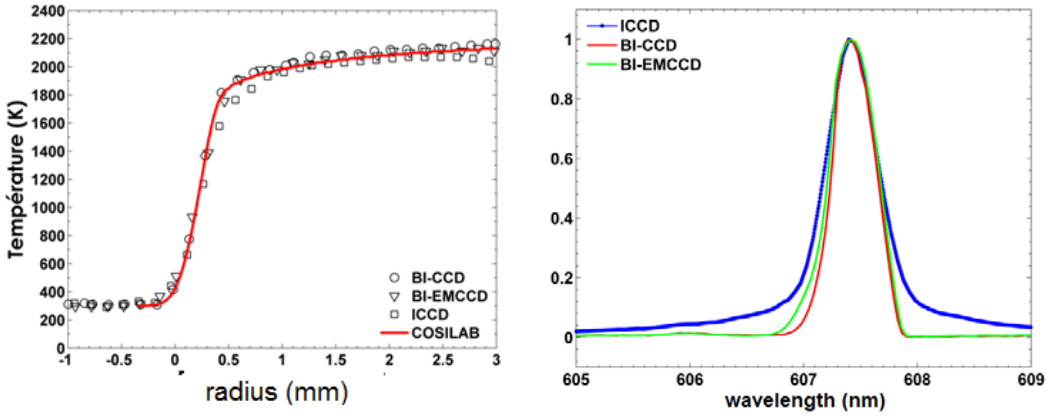

Fig 3 temperature profiles obtained from averaged SRS spectra for the three detectors

Figure 4 shows an example of single-shot Raman spectra with a spatial resolution of 160 µm, obtained on the axis of the collection system at BG for the three detectors, illustrating their different nature of noise. The two spectra acquired with the BI-EMCCD and BI-CCD show the SRS signal of the rovibrational bands of CO_2, N_2 and H_2O (Fig. 4 a, b). The possibility of measuring single-shot temperature from SRS has been demonstrated in previous work using BI-CCD camera with a PCS shutter (Ajrouche et al, 2009, 2014) (Lo et al, 2013). Here the single-shot temperature

measurements from BI-CCD, BI-EMCCD and ICCD are compared and analyzed in terms of uncertainty and accuracy. The temperature is determined by simulating the vibration-rotation spectra of N_2 by theoretical spectra. These spectra are calculated and convoluted with the in-situ instrumental functions (Lo et al, 2012) (Ajrouche et al, 2014). The SNR values obtained from single-shot spectra are defined as the ratio of peak Raman intensity of fitted spectra, considered as the "true" signal value, divided by the root-mean-square (rms) fluctuations of the difference between experimental and fitted spectra calculated in the wavelength range of the SRS signal.

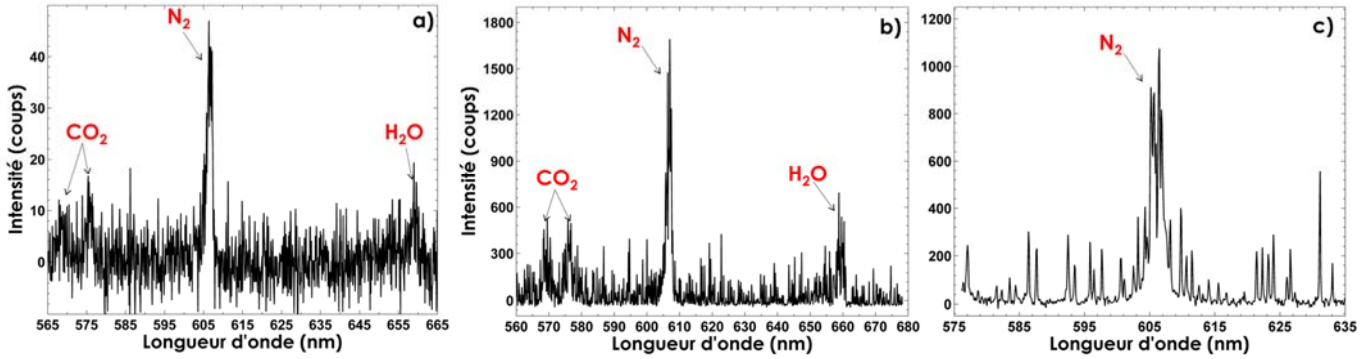

Fig 4*:* Samples of single shot Raman spectra acquired in stoichiometric methane-air flame with 160 µm spatial resolution (2130 K) using (a) BI-CCD (b) BI-EMCCD (c) ICCD

Figure 4 shows that the single-shot spectra obtained with BI-CCD and BI-EMCCD are weakly noisy, SNR of 9.92 and 8.89 respectively, and very reproducible from one shot to another. While instantaneous spectra acquired with ICCD is altered by shot noise, and varies from one shot to another. Here, SNR of 5.84 much lower than for the 2 other camera is noticed. The reproducibility of the single-shot spectra is weaker with the ICCD camera than with BI-CCD (Fig5).

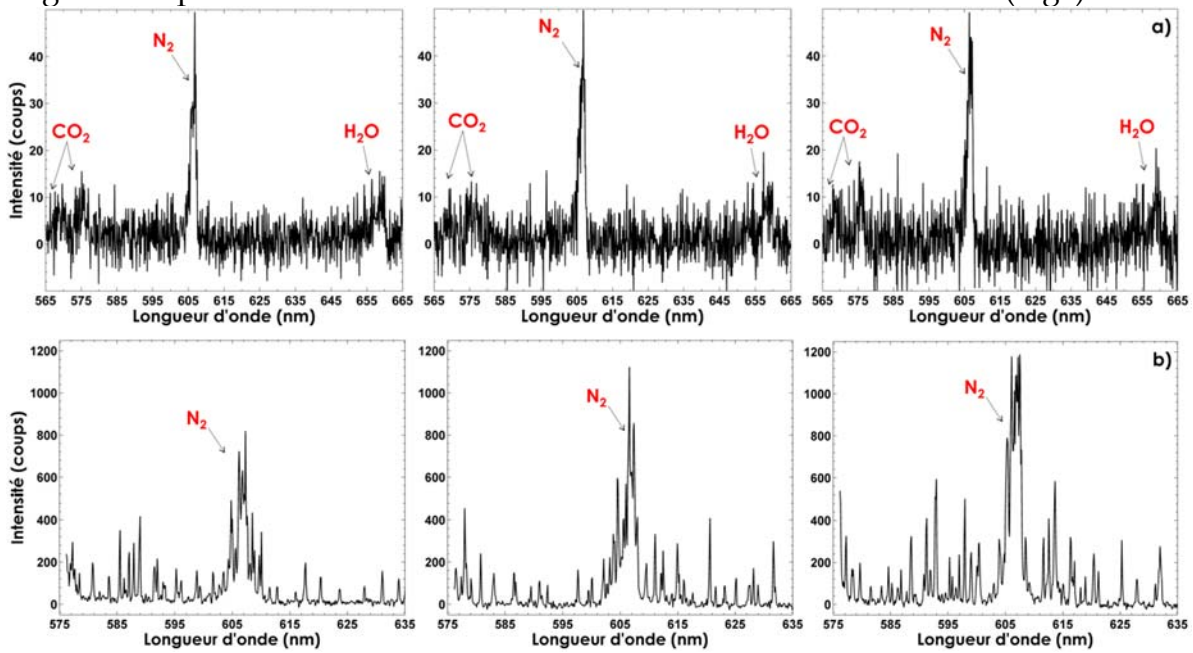

Fig 5 Samples of single shot Raman spectra acquired in stoichiometric methane-air flame with 160 µm spatial resolution (2130 K) using (a) BI-CCD (b) ICCD

Fig. 6 shows temperature PDF from stoichiometric methane-air flame, measured with the 3 detectors at BG. The average temperatures measured are 2140K, 2131K for BI-EMCCD and BI-CCD respectively. They are very close to the temperature calculated by adiabatic flame modeling COSILAB (2136K) and demonstrate that the combustion can be considered almost adiabatic in this area. In the following, the COSILAB modeling will be considered to provide the reference data (temperature and major species) of the flame. The comparison of temperature accuracy between the BI-EMCCD and BI-CCD detectors highlights their ability to provide accurate temperature measurements with an error smaller than 1% and shows the reliability and the reproducibility of experimental procedure proposed. Temperature fluctuations are almost equal for these two detectors with slight higher uncertainties obtained with BI-EMCCD (160K) than those with BI-CCD (120K). We can point out that when BI-EMCCD gain is set to 1 similar fluctuation levels (124K) to those with the standard BI-CCD are obtained. For ICCD, the temperature measurements are clearly affected by the higher NF of this device degrading the SNR from 9.92 with BI-CCD to 5.84 with ICCD and resulting in an average temperature of 1926K clearly smaller than the calculated temperature (2136K) and very high uncertainties (340K). This is due to the decrease in the spectral resolution of the vibrational bands because of the higher pixel size and the higher shot noise of this detector. Figure 7 shows the dispersion of the instantaneous temperature measurements with the ICCD camera and the loss of accuracy of the modeling for the highest vibrational bands due to the larger apparatus function of this camera (Fig 3) and the low signal-to-noise ratio at the low signal levels.

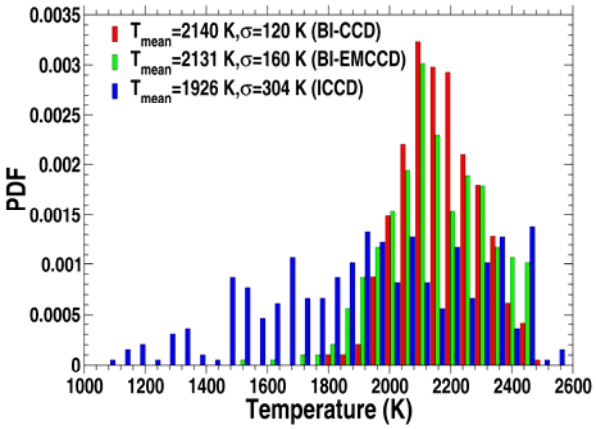

Fig 6 Temperature measurements with the 3 detectors at BG with 160µm. spatial resolution in a stoichiometric methane-air flame

Figure 8 compares averaged single-shot temperature to the calculated profile for the three detectors. In Fig3 the SRS spectra are fitted after averaging of the spectra, while in Fig 8 the instantaneous spectra are fitted and then the instantaneous temperatures are averaged.

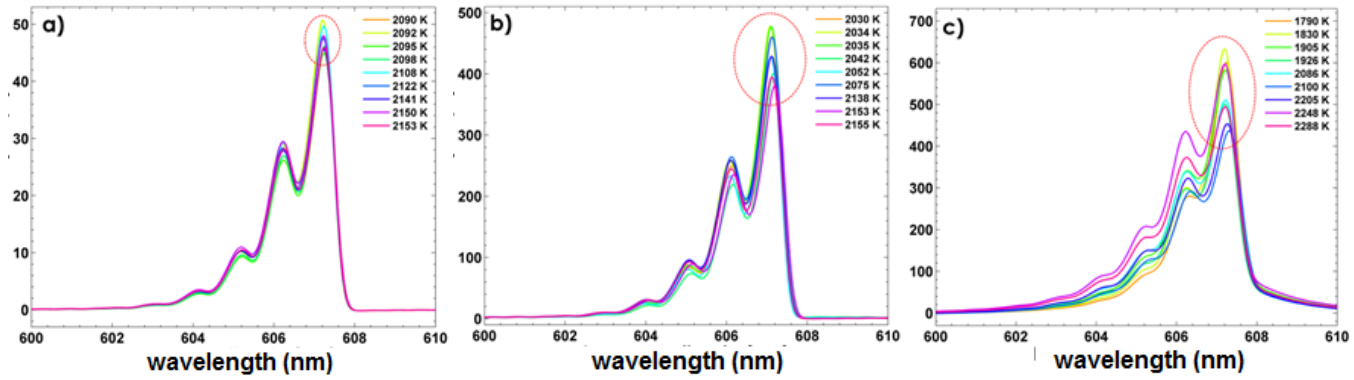

Fig 7 examples of instantaneous fitted SRS spectra of N2 for (a) BI-CCD (b) BI-EMCCD (c) ICCD

The profiles in Fig 8 obtained from both BI-CCD and the BI-EMCCD at 160 µm spatial resolution are in agreement with the COSILAB calculations. The profiles fit well with the modeling with a maximum shift at the inflexion point of 50 K for BI-EMCCD, which is reduced to 24 K for BI-CCD. The comparison of temperature accuracy between the BI-EMCCD and BI-CCD detectors highlights their ability to provide accurate temperature measurements with an error smaller than 1% and shows the reliability and the reproducibility of experimental procedure proposed. Temperature fluctuations are almost equal for these two detectors with slight higher uncertainties obtained with BI-EMCCD (160K) than those with BI-CCD (120K). We can point out that when BI-EMCCD gain is set to 1 similar fluctuation levels (124K) to those with the standard BI-CCD are obtained.

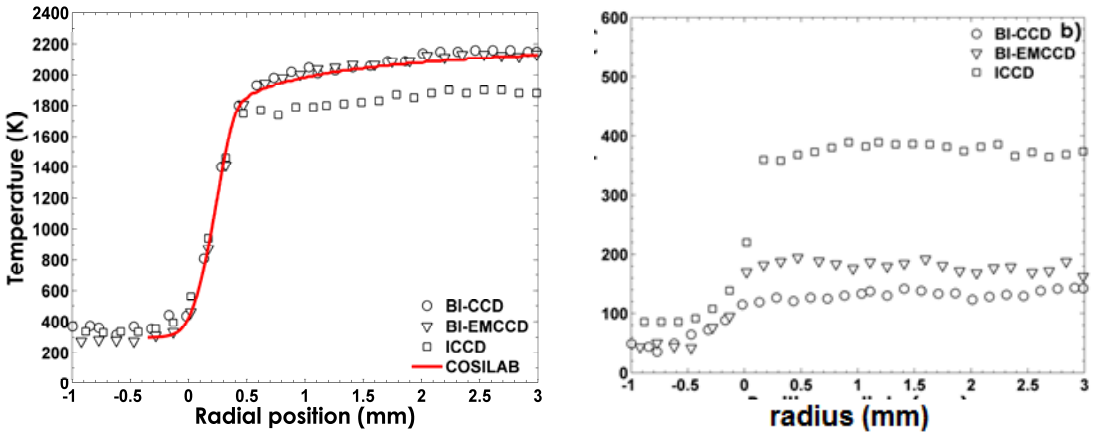

Fig 8 400-shot averaged radial profiles of temperature and temperature fluctuations from stoichiometric methane-air flame, measured by the three detectors at FG compared to temperature values calculated by COSILAB.

For ICCD, the temperature measurements are clearly affected by the higher shot-noise and the higher NF of this device degrading the SNR from 9.92 with BI-CCD to 5.84 with ICCD and resulting in an average temperature of 1926K clearly smaller than the calculated temperature (2136K) and very high uncertainties (340K).

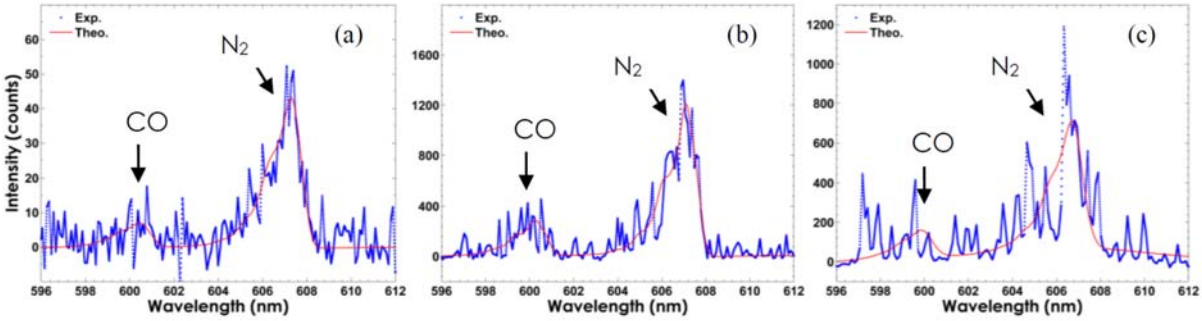

Fig9 Example of single shot N2 and CO Raman intensities in premixed methane-air flame Φ=1.4 (blue points). The solid red curve is the theoretical best-fit obtained for BI-CCD (a) BI-EMCCD (b) and ICCD (c)

The concentration measurements are also compared first for N_2, a species providing the highest signal levels, and secondly for CO in the Φ=1.4 flame, providing very low signal levels. Figure 9 presents an example of single shot SRS spectra of N_2 and CO acquired in burnt gases (160 µm spatial resolution) recorded with each camera, with their respective SRS model fit.

Density is determined using the area of theoretical spectra and the fitted temperature:

$$N^{N_2} = N_{ref}^{N_2} \frac{\int_0^\infty S_{SRS}^{N_2}(\lambda,T)d\lambda}{\int_0^\infty S_{SRS}^{N_2}(\lambda,T_{ref})d\lambda} \frac{\sum_{v,J}\sum_{QSO} f_{v,J}(T_{ref})\left(\frac{\partial\sigma}{\partial\Omega}\right)_{v,J\overrightarrow{QSO}v',J'}^{N_2}}{\sum_{v,J}\sum_{QSO} f_{v,J}(T)\left(\frac{\partial\sigma}{\partial\Omega}\right)_{v,J\overrightarrow{QSO}v',J'}^{N_2}} \quad (1)$$

$$N^{CO} = N_{ref}^{N_2} \frac{\int_0^\infty S_{SRS}^{CO}(\lambda,T)d\lambda}{\int_0^\infty S_{SRS}^{N_2}(\lambda,T_{ref})d\lambda} \frac{\sum_{v,J}\sum_{QSO} f_{v,J}(T_{ref})\left(\frac{\partial\sigma}{\partial\Omega}\right)_{v,J\overrightarrow{QSO}v',J'}^{N_2}}{\sum_{v,J}\sum_{QSO} f_{v,J}(T)\left(\frac{\partial\sigma}{\partial\Omega}\right)_{v,J\overrightarrow{QSO}v',J'}^{CO}} \quad (2)$$

Table 1 provides the concentration measurements in GB: average, fluctuations, and accuracy obtained by comparison with the adiabatic number density calculated by COSILAB, and Fig. 10 shows the results obtained when crossing the flame front in GF. Density values obtained with BI-CCD are very close to the density calculated by adiabatic flame modeling COSILAB (2.48x1018 cm-3). Density obtained with BI-EMCCD is slightly underestimated due to the higher uncertainty of temperature with this detector. For ICCD, the underestimation and uncertainties of density measurements are high.

Table 1 average number densities measured in GB with the temperature determined simultaneously by SRS model

Détecteur	**BI-CCD**	**BI-EMCCD**	**ICCD**
Densité x10^{18}molécules.cm^{-3}	2.483	2.623	3.95
Incertitudes (%)	9.2	14.5	26.5
Précision (%)	99.8	94.2	76.1

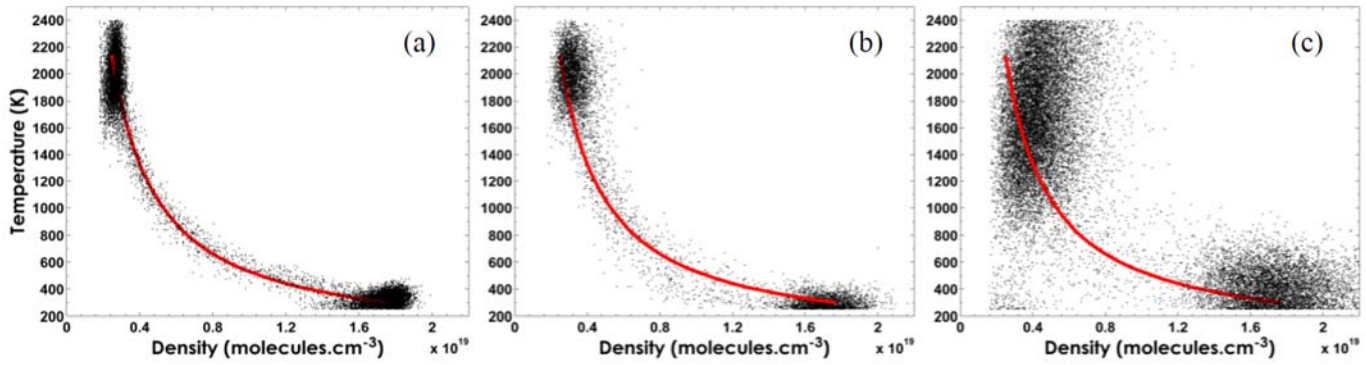

Fig 10 Scatterplots of instantaneous measurements of temperature versus density of N_2 at front flame with a probe volume of 160µm for different detectors: BI-CCD (a) BI-EMCCD (b) and ICCD (c) compared to laminar flame calculation (solid red curve)

Scatterplots of instantaneous temperature measurements versus density of N_2 when crossing the flame front (Fig. 10) show that the BI-CCD measurements reproduced well the hyperbolic behavior. The dispersion of 9.5% from either side of the modeled curve is acceptable especially if we consider the small probe volume (160 µm). This small spatial resolution, which leads to low signal levels with our experimental setup, has been chosen for the assessment of the detectors with low signal-to-noise ratio conditions. Results with a probe volume of 300 µm (Fig 11) show the decrease in dispersion of the data (6.7%). The number density measurements performed with BI-EMCCD present approximately similar results to those obtained with BI-CCD with higher dispersion of the values due to the higher uncertainties of temperature measurements performed with BI-EMCDD (Fig. 10b).

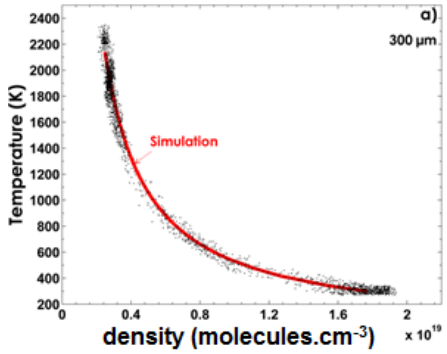

Fig 11 Scatterplots of instantaneous measurements of temperature versus density of N_2 at front flame for different detectors: BI-CCD with a probe volume of 300 µm

The scatterplot dispersion of N_2 density measurements performed with ICCD (Fig. 10c) is very broad due to the cumulated uncertainty of density and temperature measurements. That results from the false temperature determination with the modeled spectra as shown in Fig 8. To estimate the contribution of the area and temperature measurements in the error of number density,

concentration measurements in GB, where temperature is known, are performed by using the temperature value given by COSILAB (Table 2). The accuracy of the average values is clearly enhanced but it remains low for the ICCD camera, showing that the high level of noise of this detector has an impact even on the area measurement of the SRS peak.

Table 2 average number densities measured in GB with the temperature calculated by COSILAB

Détecteur	**BI-CCD**	**BI-EMCCD**	**ICCD**
Densité x10^{18}molécules.cm^{-3}	2.481	2.46	2.56
Incertitudes (%)	8.5	11.2	17.5
Précision (%)	99.9	99.2	96.8

To assess the detector for very low signal levels, CO number density are measured in GB. In fig 9a acquired from BI-CCD, the CO peak of few counts (~5) is difficult to distinguish with a SNR value of 0.92 (Table 3). The small peak value of CO obtained with BI-CCD can be embedded for some single shot spectra in the background signal and therefore information about CO will be lost. The improvement in BI-EMCCD signal quality is immediately noticeable in Fig 9b. BI-EMCCD can detect very low CO signal. For ICCD, the high shot noise decreases drastically the SNR of the CO peak to 0.84, and makes the detectability of the peak very low. We have to remember here that CO density measurement by SRS is not usual due to the low level of signal and that this issue is enhanced here by the small probe volume (160 μm).

Table 3 representative SNR of detectability, measured density of CO, accuracy and uncertainties obtained in methane-air premixed flame (Φ=1.4) in GB for different detector.

Detector	**BI-CCD**	**BI-EMCCD**	**ICCD**
SNR (160μm)	0.92	1.49	0.84
Density x10^{17}cm^{-3}(160μm)	3.02	2.89	3.35
Uncertainties (x10^{17}cm^{-3})	1.54	1.03	2.22
Accuracy (%)	3.7	0.6	15
Density x10^{17}cm^{-3}(300μm)	2.92		3.01
Uncertainties (x10^{17}cm^{-3})	1.11		1.69
Accuracy (%)	0.3		3.4

4. Conclusion

In flames, where the SRS signal is embedded in continuous background radiation, different types of cameras can be used for signal detection: BI-CCD, BI-EMCCD and ICCD. BI-CCD and BI-EMCCD offer advantages for SRS measurements, due to its high quantum efficiency and limited shot-noise. However, measurements in flame with these types of cameras require the use of a fast shutter device. Here a Pockels cell shutter PCS is used as optical gating for BI-CCD and BI-EMCCD, in order to assess accuracy and uncertainties of SRS measurements in flames and to

compare their performances to those of ICCD cameras. Results obtained with BI-CCD and BI-EMCCD for temperature, temperature gradient, and high density are in good agreement with laminar flame calculations. Fluctuations in the measured temperature with BI-CCD and BI-EMCCD for high spatial resolution (160 μm) are below 7% in burnt gases. Temperature measurements performed with ICCD camera are not so accurate and present high uncertainties due to the high shot noise. The temperature measurements by spectrum fit is not suitable with this detector and the low signal level of SRS. The measurements with ICCD are limited to density measurements with large probe volume and must be associated to another temperature measurement than SRS proposed here, as Rayleigh scattering for instance.

PCS offers time gates comparable to ICCD, and it makes on one hand the BI-CCD, the most efficient detection systems for single-shot temperature measurements but single-shot density measurements with low detectability the measurements are readout noise limited. On the other hand, the BI-EMCCD is the powerful tool for best detectability of low concentration species such as CO. The powerful improvement for BI-EMCDD is obtained because this detector removes the readout noise detection limit by applying a low-noise gain process, to enhance the signal above the noise background. This study opens prospects for the analysis of turbulent reacting flows by simultaneous 1D measurements of temperature and concentrations of major species.

Acknowledgements

This work was supported by the Haute-Normandie Region for the PhD fellowship of H. Ajrouche.

References

Ajrouche H, Lo A, Vervisch P, Cessou A (2015) Assessment of a fast electro-optical shutter for 1D spontaneous Raman scattering in flames. Measurement Science and Technology 26:075501

Ajrouche H, Lo A, Vervisch P, Cessou A (2014) 1D single-shot thermometry in flames by Spontaneous Raman Scattering through a fast electro-optical shutter 17th Int Symp on Applications of Laser Techniques to Fluid Mechanics. Lisbon, Portugal,

Barlow RS (2007) Laser diagnostics and their interplay with computations to understand turbulent combustion. Proc Comb Inst 31:49-75 DOI 10.1016/j.proci.2006.08.122

Barlow, R. Wang, G. Anselmofilho, P. Sweeney, M. Hochgreb, S. , Proc. Combust. Inst. 32 (2009)

Cleon G, Stepowski D, Cessou A (2007) Long-cavity Nd : YAG laser used in single-shot spontaneous Raman scattering measurements. Opt Lett 32:3290-3292

COSILAB (2007) The Combustion Simulation Laboratory. Version 3.1 edn. Rotexo GmbH & Co. KG, Haan, Germany,

Fernandez JM, Punge A, Tejeda G, Montero S (2006) Quantitative diagnostics of a methane/air mini-flame by Raman spectroscopy. J Raman Spectrosc 37:175-182 DOI 10.1002/jrs.1462

G. Smith DG, M. Frenklach, T. Bowman, N. Moriarty, B. Eiteneer, et al., .

Gabet K, Jiang N, Lempert W, Sutton J (2010) Demonstration of high-speed 1D Raman scattering line imaging. Applied Physics B: Lasers and Optics 101:1-5

Geyer D, Kempf A, Dreizler A, Janicka J (2005) Turbulent opposed-jet flames: A critical benchmark experiment for combustion LES. Combust Flame 143:524-548 DOI 10.1016/j.combustflame.2005.08.032

Gregor MA, Dreizler A (2009) A quasi-adiabatic laminar flat flame burner for high temperature calibration.065402

Kelman JB, Masri AR (1997) Quantitative technique for imaging mixture fraction, temperature, and the hydroxyl radical in turbulent diffusion flames. Appl Opt 36:3506-3514 DOI 10.1364/ao.36.003506

Kojima J, Nguyen QV (2008) Observation of Turbulent Mixing in Lean-Direct-Injection Combustion at Elevated Pressure. Aiaa Journal 46:3116-3127 DOI 10.2514/1.37433

Lo A, Cléon G, Vervisch P, Cessou A (2012) Spontaneous Raman scattering: a useful tool for investigating the afterglow of nanosecond scale discharges in air. Applied Physics B: Lasers and Optics 107:229-242 DOI 10.1007/s00340-012-4874-3

A. Lo, H. Ajrouche, P. Vervisch, A. Cessou, Proc. Eur. Combust. Meet. (2013) 1–7

Meier W, Keck O (2002) Laser Raman Scattering in Fuel-Rich Flames : Background Levels at Different Excitation Wavelengths. Meas Sci Technol 13:741-749

Miles PC, Barlow, R.S., (2000) A Fast Mechanical Shutter for Spectroscopic Applications. Meas Sci Technol 11:392-397